



UNIVERSITY OF LEEDS

This is a repository copy of *Understanding the interaction between active sites and sorbents during the integrated carbon capture and utilization process*.

White Rose Research Online URL for this paper:
<https://eprints.whiterose.ac.uk/168390/>

Version: Accepted Version

Article:

Sun, H, Wang, Y, Xu, S et al. (8 more authors) (2021) Understanding the interaction between active sites and sorbents during the integrated carbon capture and utilization process. *Fuel*, 286 (Part 1). 119308. ISSN 0016-2361

<https://doi.org/10.1016/j.fuel.2020.119308>

© 2020, Elsevier. This manuscript version is made available under the CC-BY-NC-ND 4.0 license <http://creativecommons.org/licenses/by-nc-nd/4.0/>.

Reuse

This article is distributed under the terms of the Creative Commons Attribution-NonCommercial-NoDerivs (CC BY-NC-ND) licence. This licence only allows you to download this work and share it with others as long as you credit the authors, but you can't change the article in any way or use it commercially. More information and the full terms of the licence here: <https://creativecommons.org/licenses/>

Takedown

If you consider content in White Rose Research Online to be in breach of UK law, please notify us by emailing eprints@whiterose.ac.uk including the URL of the record and the reason for the withdrawal request.



eprints@whiterose.ac.uk
<https://eprints.whiterose.ac.uk/>

Understanding the interaction between active sites and sorbents during the integrated carbon capture and utilization Process

Hongman Sun^a, Yehong Wang^b, Shaojun Xu^{c,d}, Ahmed I. Osman^a, Gavin Stenning^e, Jianyu Han^b, Shuzhuang Sun^a, David Rooney^a, Paul T. Williams^{f,*}, Feng Wang^{b,*} and Chunfei Wu^{a,*}

^a*School of Chemistry and Chemical Engineering, Queen's University Belfast, Belfast, BT7 1NN, UK*

^b*State Key Laboratory of Catalysis, Dalian National Laboratory for Clean Energy, Dalian Institute of Chemical Physics, Chinese Academy of Sciences, Dalian, 116023, China*

^c*UK Catalysis Hub, Research Complex at Harwell, Didcot, OX11 0FA, UK*

^d*Cardiff Catalysis Institute, School of Chemistry, Cardiff University, Cardiff, CF10 3AT, UK*

^e*ISIS Neutron and Muon Source, Rutherford Appleton Laboratory, Didcot, OX11 0QX, UK*

^f*School of Chemical and Process Engineering, University of Leeds, Leeds, LS2 9JT, UK.*

* *Corresponding authors: E-mail: c.wu@qub.ac.uk (C. Wu); wangfeng@dicp.ac.cn (F. Wang); p.t.williams@leeds.ac.uk (P.T. Williams).*

Abstract

The distance between catalytic sites (Ni) and sorbents (CaO) on the performance of integrated CO₂ capture and utilization (ICCU) process is crucial important because the sorbents demonstrate a dramatic volume increase during carbonation reaction (1st stage of ICCU) and sequentially cover the catalytic sites and retard the CO₂ conversion (2nd stage of ICCU). Herein, we synthesized various Ni/CaO-based dual functional materials (DFMs) with different distances between active sites and sorbents to provide different volume spaces for the growth of CaCO₃ during the carbonation reaction. It is found that both 1%NiCaO and 10%NiCaO synthesized by a one-pot method exhibited a low CO₂ conversion (38% and 45%, respectively) and CH₄ selectivity (58% and 69%, respectively) as the distance between catalytic sites and sorbents was so close that the Ni active sites were covered by the formed CaCO₃ during carbonation reaction. With the increase of the distance by physical mixing method, the CO₂ conversion and CH₄ selectivity of 1%Ni/CeO₂-CaO-phy were largely increased to 62% and 84%, respectively at 550 °C and atmospheric pressure when captured CO₂ from 15% CO₂/N₂. This is attributed to the fact that the Ni active sites were still well dispersed on the surface of CeO₂ nanorods instead of being covered by the newly formed CaCO₃.

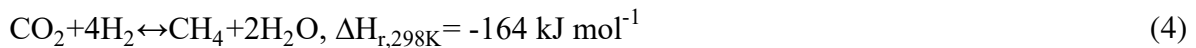
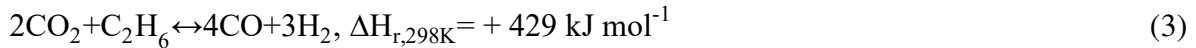
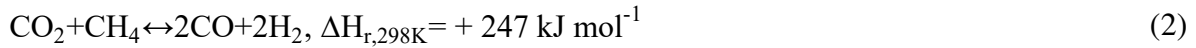
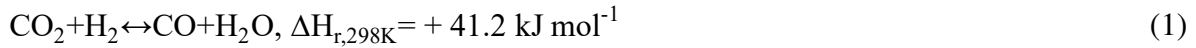
KEYWORDS: Integrated carbon capture and utilization process, dual functional materials, volume increase, active sites, methane.

1. Introduction

Reducing the concentration of atmospheric carbon dioxide (CO₂) has drawn significant attention due to the issues of global warming and serious climate change [1, 2]. CO₂ capture using CaO-based sorbents (calcium looping, CaL) is regarded as one of the most effective strategies to meet the target of reducing CO₂ emissions [3, 4]. This is because CaO-based sorbents demonstrate a high theoretical capture capacity of 17.8 mmol g⁻¹ and a low cost of \$16-44 per ton CO₂ capture, which is more competitive than that of amine scrubbing at \$32-80 per ton CO₂ capture [5, 6]. The current state-of-the-art of CaL includes CO₂ capture and sorbent regeneration in a separated reactor system with high temperature. This is not only energy-intensive but also very challenging, for example, attrition of sorbent during the transportation between carbonator and calciner [7]. Therefore, a novel integrated carbon capture and utilization (ICCU) process has been proposed, which has two stages performed in a single reactor at the same temperature as shown in Fig. S1 [8-10]. The 1st stage captures CO₂ from flue gas using sorbents and the 2nd stage converts the captured CO₂ into value-added products such as carbon monoxide (CO) and methane (CH₄) etc., by switching the feed gas to renewable H₂. This novel ICCU process will reduce the energy required for the sorbent regeneration and the infrastructure utilized in CO₂ transportation and storage [11-14].

Recently, the ICCU process combining carbon capture using CaO-based materials with the reverse water gas shift reaction (RWGS, Eq.(1)) or dry reforming of methane/ethane (Eq.(2)/Eq. (3)) has been proposed because the CaO-based materials are high-temperature sorbents for CO₂ capture [15-17]. Our previous work has successfully converted the captured CO₂ into CO at 650 °C by the ICCU process using Ni-doped CaO-based dual functional materials (DFMs) which were synthesized by a one-pot sol-gel method. The DFMs exhibited good stability for CO production after 20 cycles of the ICCU process [15]. Kim et al. proposed an ICCU process converting two major

greenhouse gases (CO₂ and CH₄) via dry reforming into a mixture of CO and H₂ by a physical mixture of CaO sorbent and Ni/MgO/Al₂O₃ catalyst[16]. The synthesized DFMs demonstrated almost full conversion of the captured CO₂ at 720 °C.



In addition, the ICCU process combining carbon capture with the Sabatier reaction (Eq. (4)) has attracted great interests due to the existence of the established infrastructure for CH₄ applications[18-20]. For example, Duyar et al. developed Ru/CaO DFMs for the ICCU process and reported a relatively low CH₄ yield of 0.5 mmol g⁻¹, which was mainly attributed to the low loading of sorbent[17]. However, the desired temperature of Ru-based catalysts for CO₂ methanation is from 200-300 °C, which is much lower than that of carbon capture using CaO-based sorbents[21]. In addition, high cost and low poisoning resistance limit the industrial application of Ru-based catalysts. Ni-based catalysts could be promising candidates in the proposed ICCU process not only because they are cost-effective, but also because they provide a match in terms of catalytic temperature for CO₂ methanation and CO₂ capture using CaO-based DFMs[22, 23].

However, using the cost-effective Ni/CaO DFMs has not been reported for the novel ICCU process to produce CH₄. Furthermore, a dramatic increase of volume from CaO (16.9 cm³ mol⁻¹) to CaCO₃ (34.1 cm³ mol⁻¹) happens after the carbonation reaction[24]. This could cause the coverage of Ni active sites by CaCO₃ and result in the insufficient conversion of the captured CO₂. Therefore, understanding the interaction between Ni active sites and CaO-based sorbents, especially the distance is essential for the design of efficient DFMs for CH₄ production during the ICCU process. In

this report, we synthesized various Ni/CaO-based DFMs with different distances between active sites and sorbents and investigated the influence of sorbent volume change during the carbonation stage on the utilization of captured CO₂. In the DFMs, Ni species are the active sites for CO₂ conversion, CaO is the sorbent used for CO₂ capture, and CeO₂ is used as a physical barrier to increase the distance between active sites and sorbents.

2. Experimental section

2.1. Materials synthesis

2.1.1. DFMs synthesized by one-pot method

The one-pot method to synthesize DFMs, predetermined amounts of Ca(NO₃)₂·4H₂O (Sigma-Aldrich), Ni(NO₃)₂·6H₂O (Sigma-Aldrich) and citric acid monohydrate (Sigma-Aldrich) acting as the chelation agent were added to deionized water at room temperature. The mixture was continuously stirred at 80 °C, dried at 120 °C overnight, and calcined at 850 °C for 2 h with a heating rate of 2 °C min⁻¹. The molar ratios of water and citric acid to Ca²⁺ were 40:1 and 1:1, respectively. The molar ratios of Ni²⁺ to Ca²⁺ were 0.01:1 and 0.1:1 for 1%NiCaO and 10%NiCaO, respectively.

2.1.2. DFMs synthesized by wet impregnation method

The wet impregnation method was used to synthesize DFMs and two types of supports in the form of CeCaO and CeCaCO₃ were used. For the synthesis of CeCaO, predetermined amounts of Ce(NO₃)₃·6H₂O (Sigma-Aldrich), Ca(NO₃)₂·4H₂O and citric acid monohydrate were added to deionized water at room temperature (The molar ratio of water, citric acid and Ce³⁺ to Ca²⁺ were 40:1, 1:1 and 0.033:1, respectively). The mixture was continuously stirred at 80 °C, dried at 120 °C overnight. The obtained products were calcined at 850 °C for 2 h with a heating rate of 2 °C

min^{-1} . CeCaCO_3 was prepared by the carbonation of CeCaO in $15\% \text{CO}_2/\text{N}_2$ (50 mL min^{-1}) at $550 \text{ }^\circ\text{C}$ for 60 min.

After the production of the two types of supports, a predetermined amount of $\text{Ni}(\text{NO}_3)_2 \cdot 6\text{H}_2\text{O}$ was dissolved into 16 mL deionized water and then 0.8 g as-prepared supports were added. The mixture was stirred at room temperature for 8 h before the evaporation of water at $80 \text{ }^\circ\text{C}$ and then dried overnight. The obtained DFMs are designated as $1\% \text{Ni}/\text{CeCaO}\text{-imp}$ and $1\% \text{Ni}/\text{CeCaCO}_3\text{-imp}$ when using CeCaO and CeCaCO_3 , respectively.

2.1.3. Synthesis of CeO_2 nanorods

CeO_2 nanorods were synthesized by a hydrothermal process as previously reported [21, 25]. Solution A (1.730 g $\text{Ce}(\text{NO}_3)_3 \cdot 6\text{H}_2\text{O}$ dissolved in 10 mL of deionized water) was added to solution B (20.0 g NaOH (Sigma-Aldrich) dissolved in 70 mL of deionized water) and the mixture was stirred for 30 min. Subsequently, the mixture was transferred into a stainless-steel auto-clave and kept at $100 \text{ }^\circ\text{C}$ for 24 h. After cooling down to room temperature, the products were filtered and washed by deionized water and ethanol until the pH reached 7. Finally, the products were dried at $80 \text{ }^\circ\text{C}$ overnight to obtain CeO_2 nanorods.

2.1.4. DFMs synthesized by physical mixing method

The physical mixing method for the synthesis of DFMs has three steps. The first step is the synthesis of CaO sorbent using a one-pot method (the detailed method is demonstrated in section 2.1.1 without the addition of Ni precursor). The second step is dispersing Ni active sites on the synthesized CeO_2 nanorods (detailed method for the synthesis of CeO_2 nanorods is described in section 2.1.3). The third step is mixing the sorbent and catalyst physically with a mass ratio of 1:1. The DFM synthesized by the physical mixing method is designated as $1\% \text{Ni}/\text{CeO}_2\text{-CaO}\text{-phy}$.

The detailed sample information is summarized in Table 1.

Table 1 Summary of sample information

Sample name	Method	NiO loading	Function
CeO ₂	Hydrothermal	/	Support and reference
CaO-CeO ₂	Physical mixing	/	Support and reference
1%NiCaO	One-pot	1%	DFMs with 1wt.% Ni
10%NiCaO	One-pot	10%	DFMs with 10wt.% Ni
1%Ni/CeCaO-imp	Wet impregnation for catalyst (Ni/CeCaO) and one-pot for support (CeCaO)	1%	DFMs promoted by Ce with 1wt.% Ni
1%Ni/CeCaCO ₃ -imp	Wet impregnation for catalyst (Ni/CeCaCO ₃) and one-pot for support (CeCaCO ₃)	1%	Carbonized DFMs promoted by Ce with 1 wt.% Ni
1%Ni/CeO ₂ -CaO-phy	Wet impregnation for catalyst (1%Ni/CeO ₂) and physical mixing with sorbent	1%	DFMs with 1wt.% Ni and physical mixed catalytic sites and sorbents

2.2. Material characterization

Powder X-ray diffraction (XRD) patterns ranging from 10 to 80° were collected by a PANalytical X'pert Highscore plus software was utilized to analyse the data. The in-situ powder X-ray diffraction patterns were measured on a Rigaku smartlab X-ray diffractometer equipped with an in-situ gas cell (Anton-paar HTK-1200N high temperature oven chamber). The measurement used the Cu K α 1 radiation (wavelength=1.5405 Å) from 3° to 90° with a scan speed of 5.5° min⁻¹. The sample was firstly reduced in 10% H₂/N₂ at 60 mL min⁻¹ for 8h, and then transferred into the in-situ gas cell. The sample was then heated to 500°C at a 5 °C min⁻¹ rate under N₂ (100 mL min⁻¹) in the cell, following pure CO₂ at a 60 mL min⁻¹ for 1 h. Transmission electron microscopy (TEM, JEOL 2010) was utilized to characterize the structure of DFMs. The samples were ultrasonically dispersed in absolute acetone and dropped cast on

carbon-coated Cu grids. High angle annular dark field (HAADF) images were carried out using a scanning transmission electron microscope (STEM, FEI Titan3 Themis 300) operating at 300 kV with FEI Super-X 4-detector EDX system. The cross-section images were performed using high-resolution scanning electron microscopy (SEM) coupled with a focused ion beam (FIB). The element distribution was collected by energy-dispersive X-ray spectroscopy (EDX). CO chemisorption performed on Micromeritics Autochem II 2920 analyser was utilized for the calculation of Ni dispersion for fresh reduced DFMs and reduced DFMs after the carbonation reaction. The samples, around 100 mg, were placed into a U-shape quartz tube and reduced at 350 °C in 5% H₂/N₂ for 30 min. After reduction, the temperature was further increased to 450 °C to remove the absorbed H₂ using pure helium for 90 min. 1% CO/He and He were used for the loop gas and carrier gas, respectively during the pulse chemisorption at 35 °C. The regulation for setting the reduction temperature for CO chemisorption is displayed in Fig. S2. A thermogravimetric analyzer (TGA, SDT Q600) was utilized to measure the weight percentage change during the ICCU process.

2.3. Integrated CO₂ capture and utilization

The ICCU performance of various DFMs was performed in a vertical fixed-bed reactor under atmospheric pressure. Typically, a predetermined amount (~0.3g) of powdered DFMs mixed with 1.0 g of quartz sand was loaded into the reactor and quartz wool was used to fix the sample. A k-type thermocouple was utilized to detect the temperature of the sample. The detailed sample information used in the ICCU process is summarized in Table 1. The 1st stage (carbonation reaction) was conducted in 15% CO₂/N₂ (50 mL min⁻¹) at 550 °C for 60 min. Subsequently, the feed gas was switched to pure H₂ (50 mL min⁻¹) to convert the captured CO₂ into CH₄ at the same temperature after the reactor was purged for 5 min using pure N₂. The products of the carbon capture stage and the conversion stage were collected in gas sample bags separately and analysed by off-line gas chromatography (GC, Techcomp 7900, TCD detector, TDX-01 column) with N₂ as the internal

standard. The CO₂ capture capacity per gram of sorbent is defined as the difference between the recorded CO₂ concentrations in the outlet gas stream and a blank experiment without any CO₂ sorbent. The product yield including CH₄ yield, CO yield and CO₂ yield is defined as per gram of catalyst. The calculation of carbon balance, CO₂ conversion, and CH₄ selectivity are described as follows:

$$\text{Carbon balance} = \frac{\text{CH}_4 \text{ yield} + \text{CO}_2 \text{ yield} + \text{CO yield}}{\text{CO}_2 \text{ capture capacity}} * 100\% \quad (5)$$

$$\text{CO}_2 \text{ conversion} = \frac{\text{CH}_4 \text{ yield} + \text{CO yield}}{\text{CO}_2 \text{ capture capacity}} * 100\% \quad (6)$$

$$\text{CH}_4 \text{ selectivity} = \frac{\text{CH}_4 \text{ yield}}{\text{CH}_4 \text{ yield} + \text{CO yield}} * 100\% \quad (7)$$

3. Results and discussion

3.1. Characterization of fresh materials

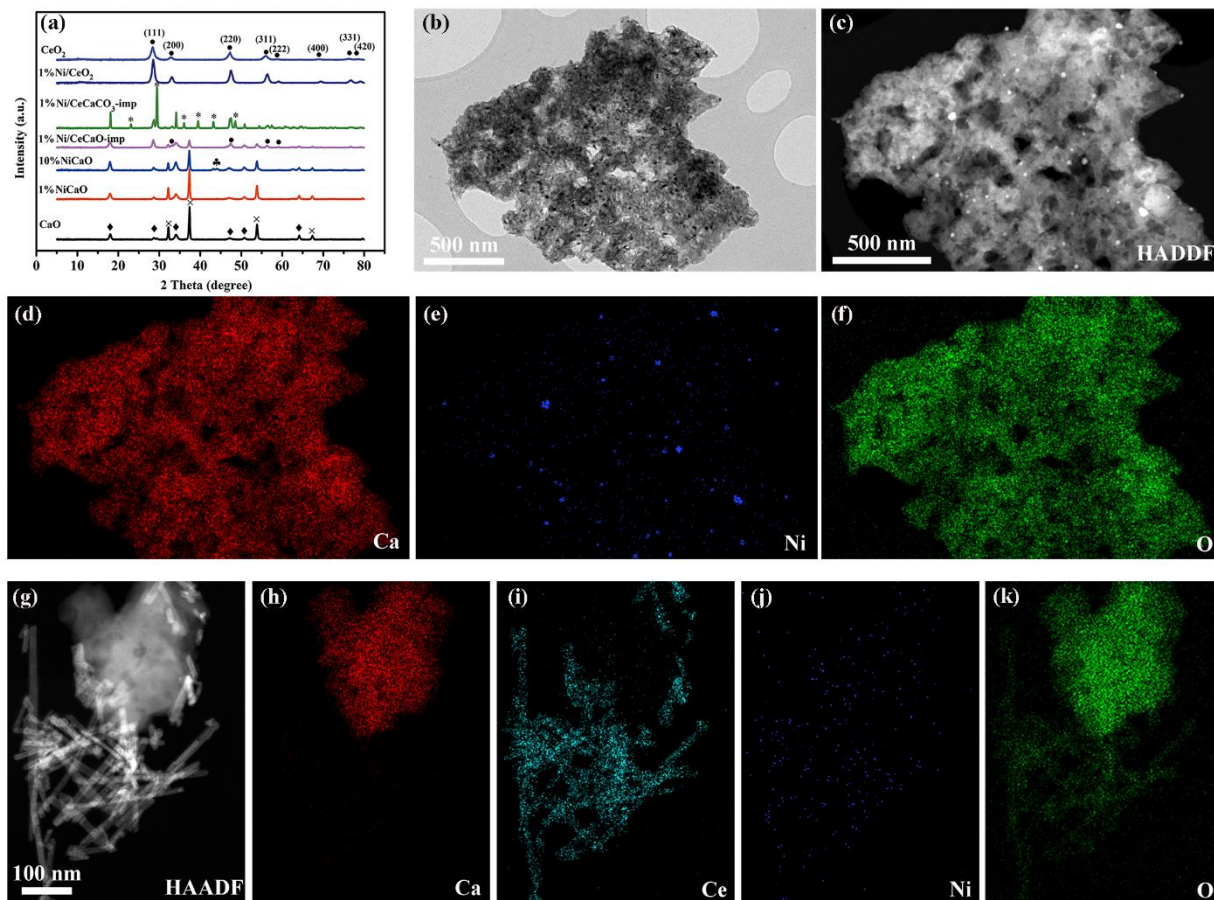


Fig.1.(a) XRD patterns of sol-gel CaO, pristine CeO₂ nanorods and various DFMs (×: CaO; ◆: Ca(OH)₂; ●: CeO₂; *: CaCO₃; ♣: Ni); HAADF-STEM images and EDX elemental mappings of (b-f) 1%NiCaO and (g-k) 1%Ni/CeO₂-CaO-phy.

The XRD patterns of sol-gel CaO, pristine CeO₂ nanorods and various DFMs with different porous structures are displayed in Fig.1. The diffraction peaks centred at 32.1°, 37.3°, 53.8°, and 67.4° are attributed to the cubic structure of CaO with space group Fm-3m[26]. The diffraction peaks centred at 18.8°, 28.7°, 34.1°, 47.1°, 50.8°, 54.4°, 59.4°, 62.6°, 64.2°, and 71.8° are assigned to the hexagonal structure of Ca(OH)₂ with space group P-3m1[27]. Thus, the CaO-based sorbent used in the ICCU process is a mixture of CaO and Ca(OH)₂. Both phases exhibit an increase of volume during the carbonation reaction due to the fact that the volume of CaCO₃ is larger than that of both CaO and Ca(OH)₂. As for 1%NiCaO, no distinct diffraction peaks attributed to Ni or NiO are observed in Fig.1. However, we confirm that Ni had been successfully introduced in porous CaO as shown in the HAADF-STEM results (Fig.1b and c), which is in agreement with the uniform distribution of Ni in EDX elemental mapping as shown in Fig 2e. In addition, it is obvious that the 1%NiCaO displays a short distance between active sites and sorbents sites. With the increase of Ni loading, a diffraction peak centred at 44.3° attributed to Ni is detected in the 10%NiCaO due to a bigger particle size as shown in Fig. S3. For the samples with the introduction of Ce, the diffraction peaks at 28.5°, 33.2°, 47.6°, 56.5°, 59.2°, 69.4°, 76.7° and 79.1° are assigned to CeO₂[28]. It is found that Ce acts as a physical barrier to provide a longer distance than one-pot method synthesised DFMs (Fig. S4). For 1%Ni/CeCaCO₃-imp, sharp peaks centred at 23.1°, 29.4°, 36.1°, 39.5°, 43.2° and 48.7° are assigned to CaCO₃. Even though no peaks belonging to Ni or NiO can be observed in 1%Ni/CeO₂, the HAADF-STEM images and EDX elemental mappings as shown in Fig 2g-k indicates that Ni species are well dispersed on the surface of the CeO₂ nanorods[29]. Compared to 1%NiCaO and

1%Ni/CeCaO-imp, a longer distance of 1%Ni/CeO₂-CaO-phy can be observed in Fig. 1g. Therefore, it is confirmed that 1%NiCaO, 10%NiCaO, 1%Ni/CeCaO-imp, 1%Ni/CeCaCO₃-imp and 1%Ni/CeO₂-CaO-phy consist of CaO and Ni acting as the sorbent and active sites, respectively.

3.2. ICCU performance of DFMs synthesized by one-pot method

The ICCU performance including product distribution, carbon balance, CO₂ conversion and CH₄ selectivity of various DFMs with different distances between active sites and sorbents is presented in Fig. 2 and Table 2. The pristine CeO₂ nanorods demonstrate a carbon capture capacity due to their basic property as reported in the previous literature [28, 30]. However, both CH₄ and CO cannot be detected indicating the ICCU process cannot occur in a single reactor at the same temperature (550 °C) using CeO₂ as both the sorbent and catalyst. When the DFMs are a physical mixture of CeO₂ nanorod and CaO, the capacity of carbon capture is greatly increased to 14.94 mmol g⁻¹. However, no CH₄ is observed after switching the feed gas to H₂ as shown in Fig. 2a due to the absence of Ni active sites. CO is the main product using the above DFMs; this might be because oxygen vacancies in the CeO₂ could directly reduce CO₂ to form CO [15, 31]. In addition, CaO-CeO₂ exhibits a relatively low carbon balance (48%) and CO₂ conversion (39%) as shown in Fig. 2b indicating more captured CO₂ is in the form of CaCO₃ (not converted during the utilization stage). This is further confirmed by the CaCO₃ diffraction peaks centred at 29.4°, 39.4° and 48.4° in the XRD results as shown in Fig. 2c.

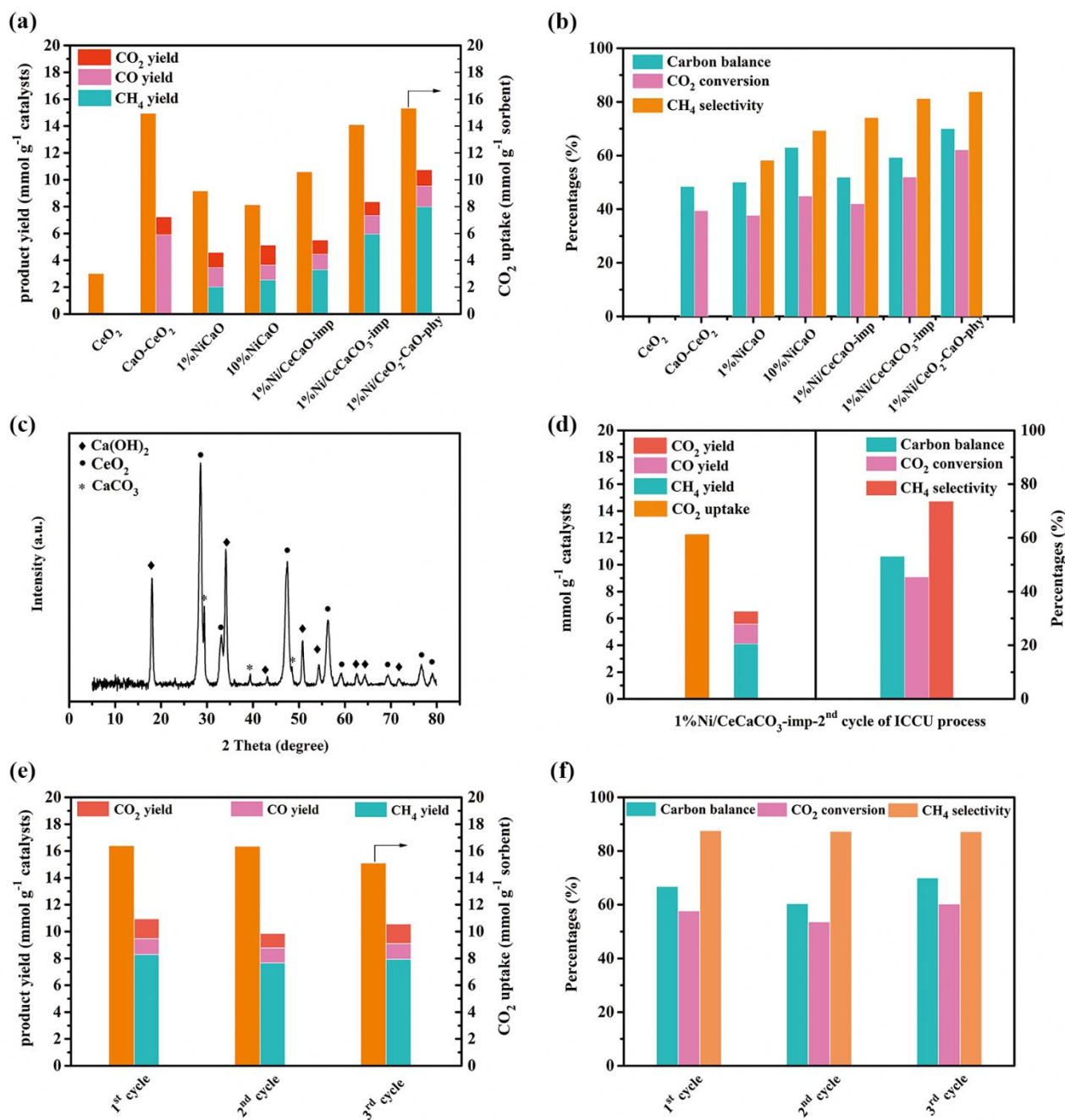


Fig.2. (a) Product distribution; (b) carbon balance, CO₂ conversion and CH₄ selectivity for ICCU performance; (c) XRD patterns of spent CaO-CeO₂ after 1 cycle of ICCU process; (d) the 2nd cycle ICCU performance of 1%Ni/CeCaCO₃-imp; (e) Product distribution; (f) carbon balance, CO₂ conversion and CH₄ selectivity for 3 cycles ICCU performance of 1%Ni/CeO₂-CaO-phy.

When using the one-pot method synthesized 1%NiCaO as the DFMs, the carbon capture capacity is 9.16 mmol g⁻¹. However, the CH₄ yield and CO₂ conversion are only 2.0 mmol g⁻¹ and 38%, respectively. The CH₄ selectivity reaches 58% indicating that the introduction of Ni species is efficient for hydrogen dissociation[32, 33]. With the further increase of Ni loading to 10 wt.% (10%NiCaO), the CH₄ yield is slightly increased from 2.0 mmol g⁻¹ to 2.5 mmol g⁻¹. The CO₂ conversion and CH₄ selectivity are also slightly increased to 45% and 69%, respectively. A large amount of captured CO₂ remains in the DFMs in the form of CaCO₃, which is proved by the XRD results in Fig. S5. This is surprising, as the increase of Ni loading is known to significantly enhance CH₄ production from CO₂ hydrogenation[33]. This might be because the volume of CaCO₃ is 34.1 cm³ mol⁻¹, which is much larger than that of CaO (16.9 cm³ mol⁻¹)[6, 34]. For the DFMs synthesized by a one-pot method, the expansion of the sorbent after carbonation reaction results in two main structural changes. On one hand, the pores of DFMs will be filled. On the other hand, the Ni active sites could be covered by the formed CaCO₃ layer. This is further confirmed by the Ni dispersion decreasing from 1.66% and 0.23% to 0.23% and 0.07% in 1%NiCaO and 10%NiCaO, respectively (Table 2).

3.3. ICCU performance of DFMs synthesized by wet impregnation

It is suggested that a short distance between sorbents and active sites in the one-pot synthesized Ni/CaO will cover the catalytic Ni sites after the carbonation stage. We prepared Ni-based catalyst by impregnating Ni sites on the support, resulting in longer distance than the one-pot reduced catalysts. As a result, the CH₄ yield of 1%Ni/CeCaO-imp synthesized by the wet impregnation method is increased to 3.3 mmol g⁻¹. This could also be attributed to the introduction of CeO₂ acting as a

physical barrier between active sites and sorbents mitigating the influence of molar volume increase of CaO during the carbonation stage [35, 36].

To further prove the negative influence of molar volume growth of CaO on CH₄ production in the ICCU process, we directly compared two DFMs consisting of Ni, Ce and Ca using 1%Ni/CeCaO-imp and 1%Ni/CeCaCO₃-imp. The sorbent of DFM, CeCaO, was carbonized prior to the impregnation of Ni active sites. In this case, the prepared catalyst, 1%Ni/CeCaCO₃-imp, has most of the Ni active sites outside of the sorbents. While for the 1%Ni/CeCaO-imp DFM, after carbonation, active Ni sites could be largely covered by CaCO₃. The Ni dispersion of 1%Ni/CeCaO-imp decreases from 0.82% to 0.21% after carbonation reaction (Table 2). As expected, CH₄ yield and CH₄ selectivity were largely increased to 6.0 mmol g⁻¹ and 81%, respectively, for the 1%Ni/CeCaCO₃-imp DFM, because the Ni active sites are not covered by CaCO₃. It is consistent with that only a slight change of Ni dispersion before (0.61%) and after carbonation reaction (0.51%). However, after 2nd cycle of ICCU using this DFM (1%Ni/CeCaCO₃-imp), CH₄ yield and CH₄ selectivity are decreased to 4.11 mmol g⁻¹ and 74%, respectively as shown in Fig. 2d. This is because during the utilization stage of the 1st cycle, CaCO₃ was decomposed to CaO, which was carbonized at the 2nd CO₂ capture stage, and covered Ni active sites at the 2nd cycle due to the molar volume change.

Table 2 ICCU performance of various DFMs.

Samples	CO ₂ capture capacity (mmol g ⁻¹)	CH ₄ yield (mmol g ⁻¹)	CO ₂ conversion (%)	CH ₄ selectivity (%)	Ni dispersion ^a (%)	Ni dispersion ^b (%)	TOF ^c (s ⁻¹)
CaO-CeO ₂	14.9	0	39	0.00	/	/	/
1%NiCaO	9.2	2.0	38	58	1.66	0.23	2.4
10%NiCaO	8.1	2.5	45	69	0.23	0.07	0.9
1%Ni/CeCaO-imp	10.6	3.3	42	74	0.82	0.21	3.0
1%Ni/CeCaCO ₃ -imp	14.1	6.0	52	81	0.61	0.51	2.0
1%Ni/CeO ₂ -CaO-phy	15.3	8.0	62	84	0.82	0.86	3.6

^a Ni dispersion before 1st stage (carbonation reaction) of ICCU process.

^b Ni dispersion after 1st stage (carbonation reaction) of ICCU process.

^cTOF= Number of moles of reactant consumed/(number of active centres*reaction time).

Number of active centres=the weight of catalysts*metal loading*Ni dispersion/Ni relative atomic mass

Reaction time=60 mins

We further evaluate the interactions between catalytic sites and sorbents at the molecular level using FIB-SEM/EDX methods. The cross-section images and Ni concentrations across the particles are conducted to study the porous structure and element distribution of both the fresh and spent DFMs synthesized by wet impregnation method as displayed in Fig.3. Through the comparison of Fig.3a and Fig.3d, no large changes can be observed in the porous structure between the fresh and spent 1%Ni/CeCaO-imp. The Ni concentration of fresh 1%Ni/CeCaO-imp as shown in Fig.3b and c is gradually decreased from the surface to the internal area indicating that the wet impregnation method is a process of infiltration from the outside to the inside. However, the surface Ni concentration of spent 1%Ni/CeCaO-imp is much lower than that of fresh 1%Ni/CeCaO-imp due to the surface Ni species which were covered by the CaCO₃ formed during the carbonation reaction. An obvious

change of porous structure is displayed in Fig.3g and j. 1%Ni/CeCaCO₃-imp as shown in Fig.3c demonstrates a bulk structure because the porous structure of Ce doped sol-gel CaO has been filled by CaCO₃ after the carbonation reaction at 550 °C for 60 min during the sample preparation. After impregnating Ni on CeCaCO₃, the surface of 1%Ni/CeCaCO₃-imp exhibited a high Ni concentration as shown in Fig.3h and i. The surface Ni concentration of spent 1%Ni/CeCaCO₃-imp after the 1st cycle of the ICCU process is further increased compared to fresh 1%Ni/CeCaCO₃-imp. This is attributed to the suggestion that CaCO₃ species on the surface of spent 1%Ni/CeCaCO₃-imp are consumed through the ICCU process.

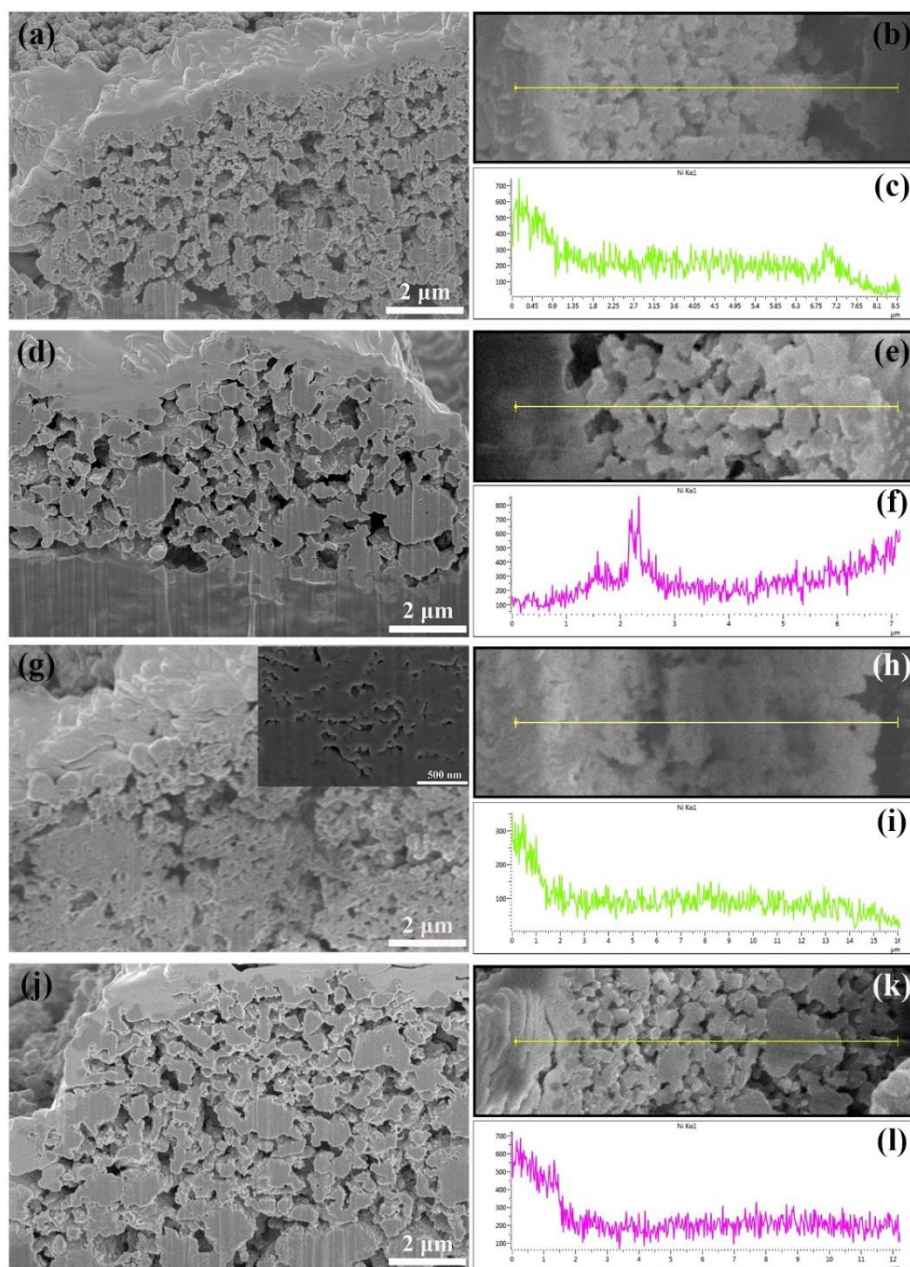


Fig.3. FIB-SEM/EDX images of various DFMs: (a-c)fresh 1%Ni/CeCaO-imp; (d-f)spent 1%Ni/CeCaO-imp; (g-i) fresh 1%Ni/CeCaCO₃-imp, (j-l) spent 1Ni/CeCaCO₃-imp.

3.4. ICCU performance of DFMs synthesized by physical mixing

As the previous developed 1%Ni/CeCaCO₃-imp cannot mitigate the negative influence of molar volume increase on the coverage of Ni sites, we developed DFMs using a physical mixing method. By physically mixing 1%Ni/CeO₂catalyst with CaO, the yield of CH₄issignificantlyincreased to

8.0 mmol g⁻¹ due to the longer distance between active sites and sorbents compared to 1%NiCaO, 10%NiCaO and 1%Ni/CeCaO-imp as shown in Fig. 1. Thus, the Ni active sites are still exposed on CeO₂ nanorods after carbonation reaction instead of being covered by the newly formed CaCO₃, which is consistent with the comparable Ni dispersion of fresh (0.82%) and carbonated DFMs (0.86%) (Table 2). Therefore, 1%Ni/CeO₂-CaO-phy exhibits the highest carbon balance (70%), CO₂ conversion (62%) as well as the highest CH₄ selectivity (84%). The highest TOF number (3.6 s⁻¹) further indicates the better catalytic performance of 1%Ni/CeO₂-CaO-phy. In addition, the 1%Ni/CeO₂-CaO-phyDFM shows a good stability after 3 cycles of ICCU as shown in Fig. 2d and f. It is proposed that the distance between Ni sites and sorbents in the physical mixed DFMs is sufficient to mitigate the problem of Ni coverage after the CO₂ capture stage. In addition, CeO₂ nanorods improve the dispersion of Ni species, and act as a support to prevent the sintering of Ni species [37, 38].

In addition, in-situ XRD patterns of 10%NiCaO and 10%Ni/CeO₂-CaO-phy were conducted to reveal the phase changes during the carbonation reaction. As shown in Fig. 4, the peaks assigned to CaCO₃ and NiO were largely increased, while the peak attributed to Ni was gradually disappeared during the carbonation reaction. We use 10%Ni/CeO₂-CaO-phy for the in-situ XRD due to a high loading of Ni is easier to be detected. However, only NiO peak can be observed in the XRD patterns. During the 2nd stage of ICCU process, NiO will be reduced by H₂ firstly for both 10%NiCaO and 10%Ni/CeO₂-CaO-phy, which can be confirmed by Ni peak centered at 44.3° in XRD results (Fig. S5 and Fig. S6). As for 10%NiCaO, most of the NiO was covered by the formed CaCO₃. Only small amount of NiO was reduced to Ni. Therefore, limited CaCO₃ reacted with the dissociated Ni and produced slight CH₄. However, the reduced Ni species are well dispersed on CeO₂ nanorods in 1%Ni/CeO₂-CaO. The ICCU performance was largely enhanced.

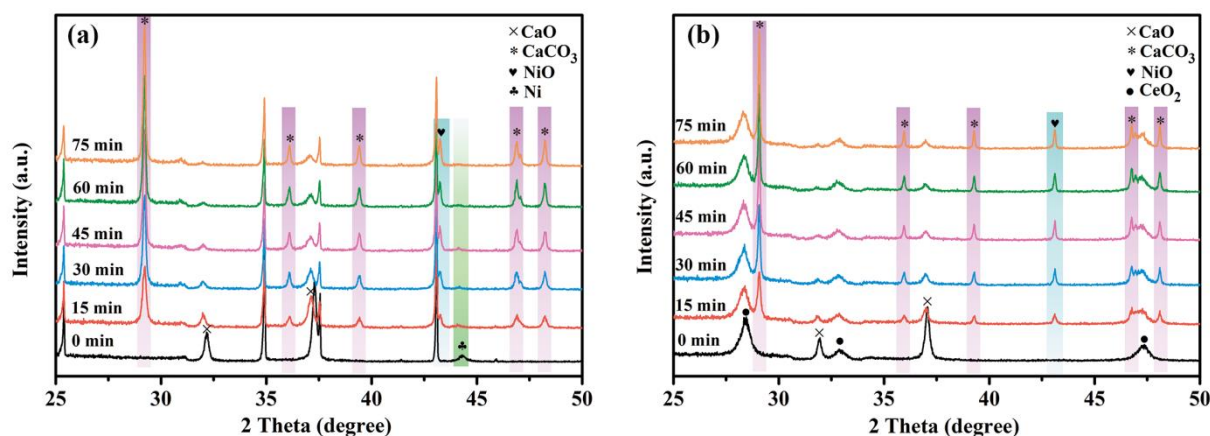


Fig.4.In-situ XRD patterns of (a) 10%NiCaO and (b) 10%Ni/CeO₂-CaO-phy during the carbonation reaction.

Based on the experimental results discussed in this work, a mechanism for the enhancement of ICCU process by 1%Ni/CeO₂-CaO-phy DFMs is proposed as shown in Fig.5. For the one-pot synthesized 1%NiCaO, the Ni active sites will be covered by formed CaCO₃ layer after carbonation reaction as shown in Fig.5a because the volume increase from CaO to CaCO₃. Therefore, 1%NiCaO exhibited a low CO₂ conversion and CH₄ selectivity. However, the ICCU performance of 1%Ni/CeO₂-CaO-phy was largely enhanced due to a longer distance between active sites and sorbents. The Ni active sites were still well dispersed on the surface of CeO₂ nanorods after carbonation reaction as shown in Fig.5b.

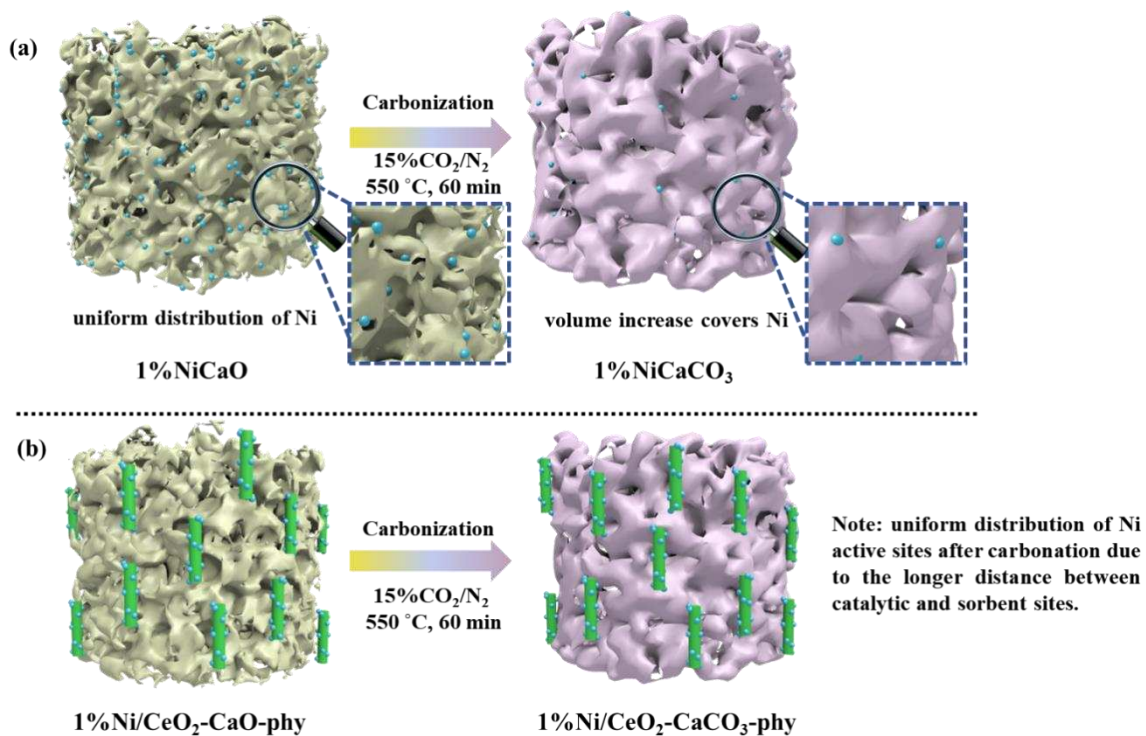


Fig.5. Proposed mechanism for the enhancement of ICCU process by 1%Ni/CeO₂-CaO-phy DFMs.

4. Conclusions

The ICCU process which is a combination of carbon capture and CO₂ methanation at 550 °C using Ni/CaO-based DFMs is proposed in this study. We further investigate the interaction between the volume increase of sorbents after the carbonation reaction and the accessibility of Ni active sites in the CO₂ conversion using various DFMs with different distances between active sites and sorbents. Compared to 1%NiCaO (CO₂ conversion and CH₄ selectivity are 38% and 58%, respectively), 10%NiCaO still exhibited a low CO₂ conversion of 45% and CH₄ selectivity of 69% due to the dramatic volume increase from CaO to CaCO₃ after the carbonation reaction. Thus, the Ni active sites in DFMs synthesized by the one-pot method were covered by the formed CaCO₃ due to the short distance between active sites and sorbents. When the DFMs were prepared by the physical mixing of CaO sorbent and Ni/CeO₂ catalyst, 1%Ni/CeO₂-CaO-phy exhibited a much better ICCU performance including a much higher CO₂ conversion (62%) and CH₄ selectivity (84%) as well as a higher

CH₄ yield (8.0 mmol g⁻¹). It is suggested that the Ni active sites are still exposed on the surface of CeO₂ nanorods instead of being covered by the newly formed CaCO₃ after the carbonation reaction. Therefore, understanding the interaction between active sites and sorbents is essential to synthesize effective DFMs for ICCU process.

CRedit authorship contribution statement

H. Sun: Conceptualization, Investigation, Visualization, Formal analysis, Writing-original draft. **Y.**

Wang: Conceptualization, Formal analysis, Writing-review & editing. **S. Xu, A. I. Osman and J.**

Han: Investigation, Writing-review & editing. **S. Sun:** Investigation, Visualization. **D. Rooney:**

Investigation, Writing-review & editing, **P. T. Williams:** Investigation, Visualization,

Writing-review & editing. **F. Wang:** Supervision, Conceptualization, Writing-review & editing. **C. Wu:**

Supervision, Conceptualization, Writing-review & editing

Conflicts of interest

There are no conflicts to declare.

Acknowledgements

The authors acknowledge the funding from the European Union's Horizon 2020 research and innovation programme under the Marie Skłodowska-Curie Grant Agreement (No. 823745).

Hongman Sun thanks the financial support from the China Scholarship Council (No. 201606450016). We would like to thank Gavin Stenning for help on the XRD instrument in the Materials Characterisation Laboratory at the ISIS Neutron and Muon Source.

References

- [1] Liu L, Das S, Chen T, et al. Low temperature catalytic reverse water-gas shift reaction over perovskite catalysts in DBD plasma. *Appl Catal B: Environ* 2020;265:118573.
- [2] Hu Y, Liu X, Zhou Z, et al. Pelletization of MgO-based sorbents for intermediate temperature CO₂ capture. *Fuel* 2017;187:328-37.
- [3] Erans M, Manovic V, Anthony E J. Calcium looping sorbents for CO₂ capture. *Appl Energy* 2016;180:722-42.
- [4] Gao N, Chen K, Quan C. Development of CaO-based adsorbents loaded on charcoal for CO₂ capture at high temperature. *Fuel* 2020;260:116411.
- [5] Perejón A, Romeo L M, Lara Y, et al. The calcium-looping technology for CO₂ capture: on the important roles of energy integration and sorbent behavior. *Appl Energy* 2016;162:787-807.
- [6] Sun H, Wu C, Shen B, et al. Progress in the development and application of CaO-based adsorbents for CO₂ capture-a review. *Mater Today Sustain* 2018;1:1-27.
- [7] Ridha F N, Lu D Y, Symonds R T, et al. Attrition of CaO-based pellets in a 0.1 MWth dual fluidized bed pilot plant for post-combustion CO₂ capture. *Powder Technol* 2016;291:60-65.
- [8] Bravo P M, Debecker D P. Combining CO₂ capture and catalytic conversion to methane. *Waste Disposal & Sustainable Energy* 2019;1:53-65.
- [9] Proaño L, Tello E, Arellano-Trevino M A, et al. In-situ DRIFTS study of two-step CO₂ capture and catalytic methanation over Ru, "Na₂O"/Al₂O₃ Dual Functional Material. *Appl Surf Sci* 2019;479:25-30.
- [10] Bermejo-López A, Pereda-Ayo B, González-Marcos J A, et al. Mechanism of the CO₂ storage and in situ hydrogenation to CH₄. Temperature and adsorbent loading effects over Ru-CaO/Al₂O₃ and Ru-Na₂CO₃/Al₂O₃ catalysts. *Appl Catal B: Environ* 2019;256:117845.
- [11] Duyar M S, Wang S, Arellano Trevino M A, et al. CO₂ utilization with a novel dual function material (DFM) for capture and catalytic conversion to synthetic natural gas: An update. *J CO₂ Util* 2016;15:65-71.
- [12] Arellano-Treviño M A, Kanani N, Jeong-Potter C W, et al. Bimetallic catalysts for CO₂ capture and hydrogenation at simulated flue gas conditions. *Chem Eng J* 2019;121953.
- [13] Sun H, Zhang Y, Guan S, et al. Direct and highly selective conversion of captured CO₂ into methane through integrated carbon capture and utilization over dual functional materials. *J CO₂ Util* 2020;38:262-72.

- [14] Sun Z, Sedghkerdar M H, Saayman J, et al. A Facile fabrication of mesoporous core-shell CaO-Based pellets with enhanced reactive stability and resistance to attrition in cyclic CO₂ capture. *J Mater Chem A* 2014;2:16577-88.
- [15] Sun H, Wang J, Zhao J, et al. Dual functional catalytic materials of Ni over Ce-modified CaO sorbents for integrated CO₂ capture and conversion. *Appl Catal B: Environ* 2019;244:63-75.
- [16] Kim S M, Abdala P M, Broda M, et al. Integrated CO₂ Capture and Conversion as an Efficient Process for Fuels from Greenhouse Gases. *ACS Catal* 2018;8:2815-23.
- [17] Duyar M S, Trevino M A A, Farrauto R J. Dual function materials for CO₂ capture and conversion using renewable H₂. *Appl Catal B: Environ* 2015;168:370-76.
- [18] Rodriguez J A, Evans J, Feria L, et al. CO₂ hydrogenation on Au/TiC, Cu/TiC, and Ni/TiC catalysts: Production of CO, methanol, and methane. *J Catal* 2013;307:162-69.
- [19] Zhen W, Gao F, Tian B, et al. Enhancing activity for carbon dioxide methanation by encapsulating (1 1 1) facet Ni particle in metal-organic frameworks at low temperature. *J Catal* 2017;348:200-11.
- [20] Martin N M, Velin P, Skoglundh M, et al. Catalytic hydrogenation of CO₂ to methane over supported Pd, Rh and Ni catalysts. *Catal Sci Technol* 2017;7:1086-94.
- [21] Guo Y, Mei S, Yuan K, et al. Low-Temperature CO₂ Methanation over CeO₂-Supported Ru Single Atoms, Nanoclusters, and Nanoparticles Competitively Tuned by Strong Metal-Support Interactions and H-Spillover Effect. *ACS Catal* 2018;8:6203-15.
- [22] Chen C, Budi C S, Wu H, et al. Size-tunable Ni nanoparticles supported on surface-modified, cage-type mesoporous silica as highly active catalysts for CO₂ hydrogenation. *ACS Catal* 2017;7:8367-81.
- [23] Solis-Garcia A, Louvier-Hernandez J F, Almendarez-Camarillo A, et al. Participation of surface bicarbonate, formate and methoxy species in the carbon dioxide methanation catalyzed by ZrO₂-supported Ni. *Appl Catal B: Environ* 2017;218:611-20.
- [24] Liu F, Li W, Liu B, et al. Synthesis, characterization, and high temperature CO₂ capture of new CaO based hollow sphere sorbents. *J Mater Chem A* 2013;1:8037-44.
- [25] Liu B, Li C, Zhang G, et al. Oxygen Vacancy Promoting Dimethyl Carbonate Synthesis from CO₂ and Methanol over Zr-Doped CeO₂ Nanorods. *ACS Catal* 2018;8:10446-56.
- [26] Sun H, Wang J, Liu X, et al. Fundamental studies of carbon capture using CaO-based materials. *J Mater Chem A* 2019;7:9977-87.

- [27] Kwasny J, Basheer P, Russell M I, et al. CO₂ sequestration in cement-based materials during mixing process using carbonated water and gaseous CO₂. 2014.
- [28] Sakpal T, Lefferts L. Structure-dependent activity of CeO₂ supported Ru catalysts for CO₂ methanation. *J Catal* 2018;367:171-80.
- [29] Wang F, Li C, Zhang X, et al. Catalytic behavior of supported Ru nanoparticles on the {1 0 0}, {1 1 0}, and {1 1 1} facet of CeO₂. *J Catal* 2015;329:177-86.
- [30] Martin D, Duprez D. Evaluation of the acid-base surface properties of several oxides and supported metal catalysts by means of model reactions. *J Mol Catal A-Chem* 1997;118:113-28.
- [31] Wang F, He S, Chen H, et al. Active site dependent reaction mechanism over Ru/CeO₂ catalyst toward CO₂ methanation. *J Am Chem Soc* 2016;138:6298-305.
- [32] Winter L R, Chen R, Chen X, et al. Elucidating the roles of metallic Ni and oxygen vacancies in CO₂ hydrogenation over Ni/CeO₂ using isotope exchange and in situ measurements. *Appl Catal B: Environ* 2019;245:360-66.
- [33] Winter L R, Gomez E, Yan B, et al. Tuning Ni-catalyzed CO₂ hydrogenation selectivity via Ni-ceria support interactions and Ni-Fe bimetallic formation. *Appl Catal B: Environ* 2018;224:442-50.
- [34] Lu H, Khan A, Pratsinis S E, et al. Flame-made durable doped-CaO nanosorbents for CO₂ capture. *Energy Fuels* 2008;23:1093-100.
- [35] Guo H, Kou X, Zhao Y, et al. Role of microstructure, electron transfer, and coordination state in the CO₂ capture of calcium-based sorbent by doping (Zr-Mn). *Chem Eng J* 2018;336:376-85.
- [36] Guo H, Kou X, Zhao Y, et al. Effect of synergistic interaction between Ce and Mn on the CO₂ capture of calcium-based sorbent: Textural properties, electron donation, and oxygen vacancy. *Chem Eng J* 2018;334:237-46.
- [37] Li M, Amari H, van Veen A C. Metal-oxide interaction enhanced CO₂ activation in methanation over ceria supported nickel nanocrystallites. *Appl Catal B: Environ* 2018;239:27-35.
- [38] Yang L, Pastor-Pérez L, Gu S, et al. Highly efficient Ni/CeO₂-Al₂O₃ catalysts for CO₂ upgrading via reverse water-gas shift: Effect of selected transition metal promoters. *Appl Catal B: Environ* 2018;232:464-71.